Proceedings of the Ninth Pacific Conference on Earthquake Engineering
Building an Earthquake-Resilient Society
14-16 April, 2011, Auckland, New Zealand

A methodology for post-mainshock probabilistic assessment of building collapse risk

N. Luco

Geologic Hazards Science Center, US Geological Survey (USGS), Golden, Colorado, USA.

M.C. Gerstenberger & S.R. Uma

GNS Science, Avalon, Lower Hutt, New Zealand.

H. Ryu, A.B. Liel & M. Raghunandan

Department of Civil Engineering, University of Colorado at Boulder, USA.

ABSTRACT: This paper presents a methodology for post-earthquake probabilistic risk (of damage) assessment that we propose in order to develop a computational tool for automatic or semi-automatic assessment. The methodology utilizes the same so-called risk integral which can be used for pre-earthquake probabilistic assessment. The risk integral couples (i) ground motion hazard information for the location of a structure of interest with (ii) knowledge of the fragility of the structure with respect to potential ground motion intensities. In the proposed post-mainshock methodology, the ground motion hazard component of the risk integral is adapted to account for aftershocks which are deliberately excluded from typical pre-earthquake hazard assessments and which decrease in frequency with the time elapsed since the mainshock. Correspondingly, the structural fragility component is adapted to account for any damage caused by the mainshock, as well as any uncertainty in the extent of this damage. The result of the adapted risk integral is a fully-probabilistic quantification of post-mainshock seismic risk that can inform emergency response mobilization, inspection prioritization, and re-occupancy decisions.

1 INTRODUCTION

1.1 Motivation

Increasingly, probabilistic seismic risk (of damage) assessment is becoming the basis for longer-term or "pre-earthquake" mitigation approaches for buildings and other structures, e.g. seismic design standards in building codes. For example, the latest edition of the American Society of Civil Engineers (ASCE) standard entitled "Minimum Design Loads for Buildings and Other Structures" (ASCE 2010) defines Risk-Targeted Maximum Considered Earthquake (MCE_R) ground motion maps for the United States (US) by explicitly targeting a probabilistic 1% risk of collapse in 50 years, an approximation of the lifespan of a building. These probabilistic risk-based maps have since been adopted for inclusion in the 2012 International Building Code (International Code Council 2012). Moreover, the next generation of performance-based seismic design procedures for new and existing buildings being developed by the Applied Technology Council (http://www.atcouncil.org/Projects/atc-58-project.html) use probabilistic risk of earthquake-caused deaths, dollars (repair costs), and downtime (repair duration) as metrics for seismic performance assessment of buildings.

1.2 Previous work

Probabilistic risk assessment has also been proposed as a basis for making shorter-term or "post-earthquake" mitigation decisions after a mainshock has occurred and when the threat of aftershocks

lingers. For example, the Advanced Seismic Assessment Guidelines developed by Bazzurro et al (2006) use the probability that an aftershock ground motion will exceed the capacity of a mainshock-damaged building (treated deterministically for simplicity) as a rational criterion for deciding whether and when to permit re-occupancy of the building. Similarly, Yeo & Cornell (2005) have developed a time-dependent building "tagging" (i.e. permitting or restricting occupancy) policy for the aftershock environment using probability of collapse as a proxy for fatality risk.

1.3 **Preview of methodology**

This paper presents the methodology for post-mainshock probabilistic risk assessment that we propose in order to develop a computational tool for automatic (or semi-automatic) assessment, with funding from the New Zealand Earthquake Commission (EQC). The methodology utilizes the same so-called risk integral (e.g., Applied Technology Council 1978, McGuire 2004) that can be used for pre-earthquake probabilistic risk assessment. As reviewed in Section 2 of the paper, the risk integral couples (i) ground motion hazard information for the location of a structure of interest with (ii) knowledge of the fragility of the structure with respect to potential ground motion intensities. In other words, the risk integral combines information about both the ground motion *demand* and the *capacity* of the structure to withstand such demand.

In the proposed post-mainshock methodology, explained in Section 3, the ground motion hazard/demand component of the risk integral is adapted to account for aftershocks which are deliberately excluded from typical pre-earthquake hazard assessments. Correspondingly, the structural fragility/capacity component is adapted to account for any damage caused by the mainshock, as well as any uncertainty in the extent of this damage. The result of the adapted risk integral is a fully-probabilistic quantification of the post-mainshock seismic risk, i.e. the risk of further damage in aftershocks. By comparing it with tolerated pre-earthquake risk levels (e.g. the 1%-in-50-years risk of collapse mentioned above in Section 1.1), the post-mainshock result can inform emergency response mobilization, inspection prioritization, and re-occupancy decisions, as discussed in Section 4.

1.4 **Applications addressed in this paper**

Although we focus on mainshock-aftershock sequences in this paper, the post-earthquake risk assessment methodology presented can be applied after any earthquake (a mainshock, aftershock, or foreshock). Furthermore, to the extent that the post-earthquake ground motion hazard component of the assessment includes the potential for so-called triggered earthquakes, the methodology can apply for sequences like the 1811-1812 New Madrid Seismic Zone earthquakes in the US and the recent 2010-2011 earthquakes near Christchurch in New Zealand (NZ).

We also focus on buildings in this paper, but analogous methodologies can be applied to other structures such as bridges and dams. While we focus on collapse risk in the sections that follow, the risk of exceeding any other state of damage can be considered with the same methodology.

2 **PRE-MAINSHOCK RISK ASSESSMENT METHODOLOGY**

2.1 **Risk integral**

Before a mainshock has occurred, and long enough after a past mainshock that the remaining threat of aftershocks is negligible, the risk of collapse of a building at a particular location can be computed via the risk integral mentioned above. As an early example, the risk integral was used in ATC 3-06 (Applied Technology Council 1978) to compute collapse risks that result from designing buildings for uniform-hazard ground motions. Recently, the risk integral has been used to revisit these ATC 3-06 computations (Luco et al 2007), and ultimately to derive the new MCE_R ground motions in (ASCE 2010) and FEMA P-750 (Building Seismic Safety Council 2009).

As expressed in Equation 1 for collapse risk, λ[Collapse], the risk integral combines a collapse fragility curve for the building of interest, Pr[Collapse|IM=a], with a ground motion hazard curve for its location, λ[IM>a]. The fragility and hazard curve are described in more detail in the next two

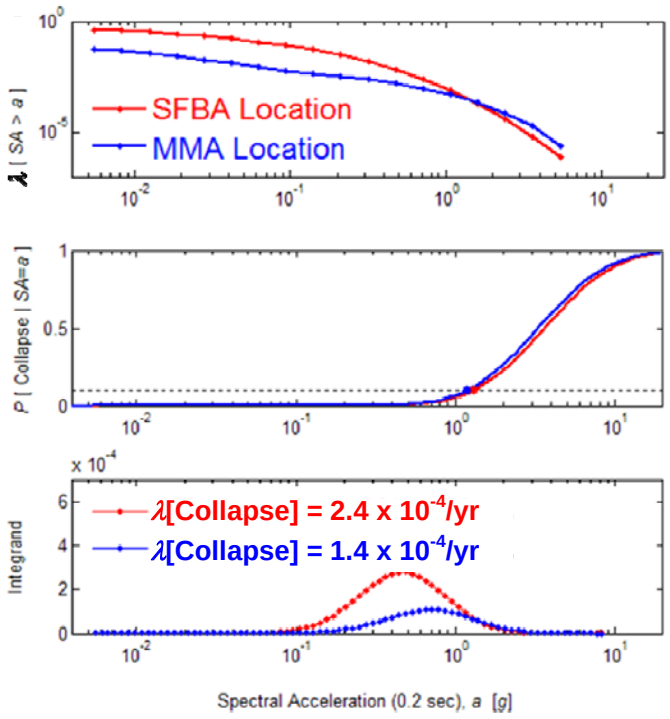

Figure 1. Illustration of the risk integral for computing collapse risk (bottom panel) via convolution of a collapse fragility curve (middle panel) with a ground motion hazard curve (top panel). The red and blue curves are for San Francisco Bay Area (SFBA) and Memphis Metropolitan Area (MMA) building locations, respectively. Each integrand curve in the bottom panel shows the product, at each ground motion intensity measure value (0.2-second spectral acceleration in this case), of the corresponding hazard curve and the derivative of the corresponding fragility curve. The area under (i.e. the integral of) each integrand curve is the collapse risk, i.e. the mean annual frequency of collapse. This figure has been adapted from (Luco et al 2007).

subsections, but in short (and loosely speaking) the fragility curve provides "what-if" probabilities of collapse for a range of potential ground motion intensity measure (IM) values, and the hazard curve provides annual probabilities of exceeding those IM values. The combination of these curves via the risk integral yields the annual (i.e. in-the-next-year) probability of collapse of the building at its particular location. Figure 1 illustrates the risk integral for two example buildings.

$$\lambda[\text{Collapse}] = \int_0^\infty \Pr[\text{Collapse} \mid \text{IM} = a] \left| \frac{\mathrm{d}\lambda[\text{IM} > a]}{\mathrm{d}a} \right| \mathrm{d}a \qquad (1)$$

In Equation 1, λ is used in denoting the collapse risk and the ground motion hazard curve because, strictly speaking, both are in terms of mean annual frequency rather than annual probability. Probabilities for other time horizons (e.g. 50 years) are commonly calculated using a Poisson probability distribution (e.g. see McGuire 2004).

2.2 **Collapse fragility curves**

As illustrated in the middle panel of Figure 1, a collapse fragility curve summarizes the probability of collapse of a building for each in a range of IM values it could be subjected to. The probability is near-zero when the IM value is relatively small, and near-unity for a relatively large IM value.

A collapse fragility curve can be developed via expert opinion, data from past earthquakes and shake table experiments, and/or computer simulations. As will be explained below in Section 3.1, for our post-mainshock risk assessment methodology we develop the collapse fragility curve via (predominantly) computer simulations, namely nonlinear response history analyses (more specifically, incremental dynamic analyses) of a building model subjected to numerous ground motion seismograms. Such analyses are already being used to derive collapse fragility curves for *pre-*

mainshock risk assessment, e.g. in FEMA P-695 (ATC 2009) and (Ryu et al 2011). In the former, the collapse fragility curves derived are for specific multi-degree-of-freedom building models, whereas in the latter they are for generic single-degree-of-freedom building models that each represent a general type of building, e.g. a mid-rise reinforced concrete moment-resisting frame building. Both and other kinds of collapse fragility curves can be used in the pre- and post-mainshock risk assessment methodologies described in this paper.

2.3 **Ground motion hazard curves**

As illustrated in the top panel of Figure 1, a ground motion hazard curve for a location summarizes the mean annual frequency (MAF) of exceeding each in a range of potential IM values. The MAF is relatively high for small IM values, and relatively low for large IM values.

In pre-mainshock hazard assessment, ground motion hazard curves are computed via Probabilistic Seismic Hazard Analysis (PSHA; Cornell 1968, McGuire 2004). PSHA combines information on potential sources of earthquakes (e.g. faults and locations of past earthquakes), potential magnitudes of earthquakes from these sources and their frequencies of occurrence, and potential ground motions generated by these earthquakes. Uncertainty and randomness in each of these components is accounted for in the combination. For a grid of locations covering the US, pre-mainshock hazard curves computed via PSHA are readily available from the USGS National Seismic Hazard Mapping Project (http://earthquake.usgs.gov/hazards/products/).

It is relevant to note that aftershocks (and foreshocks) are deliberately removed from the catalogues of historical earthquakes used for typical PSHA computations, in order to be consistent with the conventional assumption of independent (Poissonian) earthquakes in time, as opposed to mainshock-aftershock clusters. As will be summarized below in Section 3.3, we make use of an adapted version of PSHA in computing hazard curves for our *post*-mainshock risk assessment methodology.

3 **POST-MAINSHOCK RISK ASSESSMENT METHODOLOGY**

3.1 **"Post-earthquake risk integral"**

As alluded to above in the introduction, after a mainshock the risk of a building at a particular location collapsing in an aftershock can still be computed via the risk integral (Equation 1). If the building *was not* damaged by the mainshock, the only change is that the ground motion hazard curve used in the risk integral is now one that accounts for the threat of aftershocks. The aftershock hazard decreases with the time elapsed since the mainshock, however, rapidly enough that the aftershock hazard curves we use are expressed in terms of a 24-hour time period (Gerstenberger et al 2004). As a result, our "post-earthquake risk integral" computes daily probabilities (strictly speaking, mean daily frequencies) of collapse, instead of the annual probabilities commonly computed in pre-mainshock use of the risk integral. Longer post-mainshock time horizons that account for the time-varying aftershock hazard can be considered via "equivalent constant rates" proposed by Yeo & Cornell (2005).

If the building *was* damaged (but not already collapsed) by the mainshock, not only is the hazard curve used in the risk integral changed, but so is the fragility curve. The substituted fragility curve accounts for the damage caused by the mainshock, as well as any uncertainty in the extent of this damage. Our methodology for deriving such post-mainshock fragility curves is discussed in the next subsection and in the PCEE 2011 paper by Ryu et al (paper number 225).

3.2 **Post-mainshock fragility curves**

As one might expect, the fragility curves used in our post-mainshock risk assessment methodology account for any damage caused by the mainshock. This typically increases the probabilities of collapse for the considered range of potential (future) IM values, as illustrated in Figure 2. The amount of increase depends of course on the extent of the mainshock damage, which is commonly discretized into so-called damage states, e.g. none, slight, moderate, extensive, and complete in HAZUS, the US Federal Emergency Management Agency (FEMA) methodology for estimating potential losses from disasters (http://www.fema.gov/hazus/). As will be explained below, uncertainty in what damage state

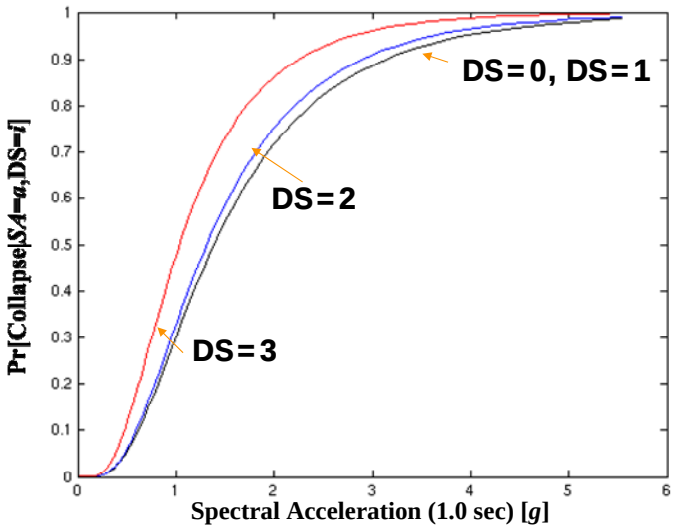

Figure 2. Example damaged-building fragility curves for certain damage states caused by the mainshock. The damage states are no damage (DS=0), onset of nonlinear behaviour in the building (DS=1), fracture of exterior beam-column connections in the first floor (DS=2), and fracture of interior connections (DS=3). As explained in the paper, if the actual damage state is uncertain (e.g. before inspection), the various fragility curves are averaged with weights corresponding to the probability of each possible post-mainshock damage state. This figure has been adapted from (Gerstenberger et al 2008).

resulted from the mainshock, e.g. due to incomplete inspection, is accounted for in our post-mainshock fragility curves.

For a certain (given) damage state caused by the mainshock, we develop a corresponding damaged-building fragility curve with a procedure proposed in (Ryu et al 2011), which is an improvement of the procedure in (Luco et al 2004). Very briefly, the procedure first generates numerous realizations of the building in the given damage state via nonlinear response history analyses (more specifically, incremental dynamic analyses) of the originally undamaged building model using numerous seismograms that represent mainshock ground motions. While the broad damage state (e.g., "moderate") is the same for each realization, the details of the state of the building are different for each realization, and the numerous realizations sample these differences. Then a fragility curve is developed for each realization of the damaged building, again via nonlinear response history analyses (incremental dynamic analyses), but now of the damaged-building model. The seismograms used in these damaged-building analyses represent aftershock ground motions (although they do not necessarily need to be recordings from aftershocks exclusively). Finally, the fragility curves for the numerous realizations are, in effect, averaged to arrive at the fragility curve for the given damage state of interest.

Uncertainty in the extent of any mainshock damage – i.e., uncertainty in the "post-mainshock damage state" – is accounted for in our methodology by applying the theorem of total probability. As expressed in Equation 2, the post-mainshock fragilty curve, Pr[Collapse|IM=a], is equal to a weighted average of the fragility curves for all of the n possible post-mainshock damage states, each denoted Pr[Collapse|IM=a,DS=i]. The respective weights are the probabilities of the possible post-mainshock damage states, Pr[DS=i], which can be determined in the three different ways that are discussed in the next three subsections.

$$\Pr[\text{Collapse} \mid \text{IM} = a] = \sum_{i=1}^{n} \Pr[\text{Collapse} \mid \text{IM} = a, \text{DS} = i] \Pr[\text{DS} = i] \qquad (2)$$

3.2.1 *ShakeMap-based post-mainshock damage state probabilities*

Promptly after an earthquake, a ShakeMap (e.g. from http://earthquake.usgs.gov/shakemap/) provides best-estimates of ground motion IM values experienced, typically based on (i) a magnitude, location, and other information about the earthquake, (ii) information about the near-surface geology of the affected region, (iii) a ground motion prediction equation like the Next Generation Attenuation (NGA) relationships for the Western US (http://peer.berkeley.edu/ngawest/), and (iv) if available, IM values from recording stations. A parallel map of the uncertainty in the IM values generated by the earthquake can also be produced, with no (or at most little) uncertainty at the recording stations. More formally, the maps provide a median and logarithmic standard deviation of the IM at each location, denoted here as m_{IM} and σ_{lnIM}, respectively.

With m_{IM} and σ_{lnIM} for the location of a building of interest, a lognormal complementary cumulative probability distribution of the IM value generated by the mainshock can be calculated according to Equation 3, where a denotes each in a range of possible IM values.

$$\Pr[\mathrm{IM} > a] = 1 - \Phi\left[\frac{\ln a - \ln m_{\mathrm{IM}}}{\sigma_{\ln \mathrm{IM}}}\right] \tag{3}$$

In order to propagate the IM probability distribution in Equation 3 into post-mainshock damage state probabilities, we slightly modify the components of the risk integral given in Equation 1. More specifically, we couple the ShakeMap-based IM probability distribution, Pr[IM>a], with a fragility curve for the pre-mainshock (or undamaged) building and the damage state of interest, Pr[DS>i|IM=a]. This combination is expressed mathematically in Equation 4.

$$\Pr[\mathrm{DS} > i] = \int_0^\infty \Pr[\mathrm{DS} > i \mid \mathrm{IM} = a] \left|\frac{\mathrm{d}\Pr[\mathrm{IM} > a]}{\mathrm{d}a}\right| \mathrm{d}a \tag{4}$$

The post-mainshock damage state probabilities, Pr[DS=i], are then calculated by using Equation 4 for both the damage state of interest (e.g., “moderate) and the next greater damage state (e.g. “severe”), i.e. Pr[DS=i] = Pr[DS>i] - Pr[DS>$i+1$]. Note that these automatable post-mainshock damage state probabilities can themselves inform emergency response mobilization, when applied to an inventory of structures. Though not via the fully-probabilistic Equation 4, the USGS ShakeCast application (http://earthquake.usgs.gov/shakecast/) delivers such information that is already used for emergency response purposes in the US. Via Equation 4 and the ShakeMap system currently being developed for NZ, our computational tool will also deliver such intermediate (to post-earthquake risk) information.

3.2.2 *Inspection-based post-mainshock damage state probabilities*

A post-mainshock inspection of a building by a structural engineer can improve upon the prompt ShakeMap-based damage state probabilities described in the preceding subsection. For example, the engineer might opine that the observed damage is fully consistent with the damage state “2” defined in the caption of Figure 2 (i.e. Pr[DS=2]=1), or that it may be indicative of damage states 2 or 3, with equal likelihood (i.e. Pr[DS=2]= Pr[DS=3]=0.5). In fact, the engineer could be asked to assign likelihoods for all of the discrete damage states identified (e.g., Pr[DS=0]=0, Pr[DS=1]=0.1, Pr[DS=2]=0.6, Pr[DS=3]=0.3). Note that this allows the engineer to first focus on the state of damage of the building, rather than the more subjective re-occupancy decision. The collapse risks that result from inputting Pr[DS=i] into Equation 2 and ultimately the risk integral (Equation 1) can subsequently inform the re-occupancy decision.

3.2.3 *Building-instrumentation-based post-mainshock damage state probabilities*

Although not discussed in detail in this paper, building instrumentation data (e.g. peak transient and/or residual roof displacements) from a mainshock can be used to determine or constrain post-mainshock damage state probabilities. For example, residual roof displacement observations can be coupled with results from the nonlinear response history analyses conducted to develop pre-mainshock fragility curves (see Section 2.2). This coupling can be accomplished via a Bayesian updating methodology.

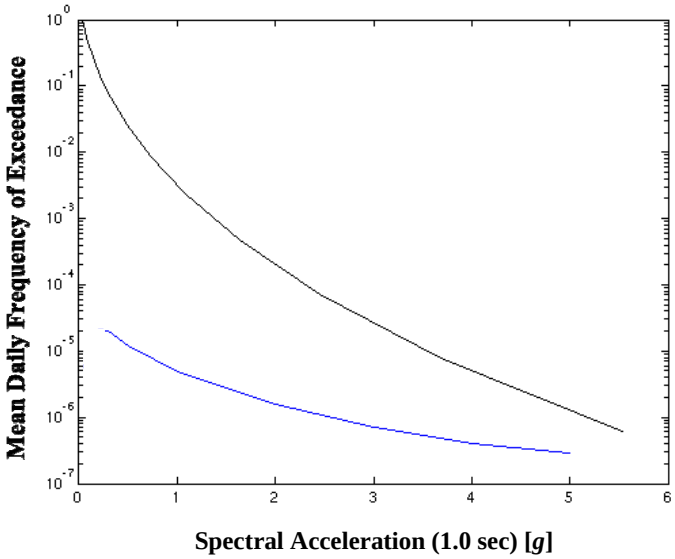

Figure 3. Example aftershock ground motion hazard curve (upper line) at a location 10km from the 1994 Northridge, California mainshock (magnitude 6.7), immediately after the earthquake. For comparison, the pre-mainshock hazard curve (lower line) for the same location is also shown. This figure has been adapted from (Gerstenberger et al 2008).

3.3 **Aftershock ground motion hazard curves**

Post-mainshock, ground motion hazard curves that account for potential aftershocks can be computed via an adaptation of pre-mainshock PSHA (described in Section 2.3). The USGS and GNS Science 24-Hour Aftershock Forecast Maps for California (http://earthquake.usgs.gov/earthquakes/step/) and NZ (http://www.geonet.org.nz/canterbury-quakes/aftershocks/), respectively, provide one point for such hazard curves via the PSHA adaptation explained in (Gerstenberger et al 2004). Full aftershock ground motion hazard curves are being computed for NZ, in near-real time, as part of our development of a computational tool for post-earthquake risk assessment. The third iteration of the Uniform California Earthquake Rupture Forecast (see http://www.wgcep.org/versions/) plans to develop an operational earthquake forecast that could, in the future, be extended to provide full aftershock ground motion hazard curves as well. As demonstrated in Figure 3, an aftershock hazard curve can be orders of magnitude higher (on the frequency of exceedance scale) than its conventional pre-mainshock counterpart, particularly immediately after the mainshock.

4 **CONCLUDING REMARKS**

4.1 **Summary of proposed methodology**

The proposed methodology for post-earthquake probabilistic risk assessment utilizes the same so-called risk integral that can be used for pre-earthquake probabilistic assessment. The risk integral couples i) ground motion hazard information for the location of a structure of interest with ii) knowledge of the fragility of the structure with respect to potential ground motion intensities. In the proposed post-mainshock methodology, the ground motion hazard component of the risk integral is adapted to account for aftershocks which are deliberately excluded from typical pre-earthquake hazard assessments and which decrease in frequency with the time elapsed since the mainshock. Correspondingly, the structural fragility component is adapted to account for any damage caused by the mainshock, as well as any uncertainty in the extent of this damage.

4.2 **Examples of potential applications**

The results of the proposed probabilistic post-earthquake risk assessment methodology can inform emergency response mobilization, inspection prioritization, and re-occupancy decisions. More

specifically, the intermediate post-mainshock damage state probabilities computed via Equation 4 for an inventory of buildings can be used in deciding where to send emergency response teams – e.g. wherever the probability is high that the post-mainshock damage state is collapse. Similarly, the post-mainshock collapse risks computed via the post-earthquake risk integral described in Section 3 can be used in prioritizing inspections of buildings that did not collapse in the mainshock but have a high risk of collapsing in an aftershock or "triggered" earthquake. The eventual inspections of individual buildings can also make use of the post-mainshock collapse risks, in making re-occupancy (e.g. red/yellow/green tag) decisions by comparing against corresponding pre-mainshock collapse risks. Note that by making use of the post-mainshock collapse risks, the re-occupancy decisions can (if desired) change with the time elapsed since the mainshock, as the frequency of aftershocks decreases and hence so do the post-mainshock collapse risks.

5 ACKNOWLEDGEMENTS

Our development of a computational tool for automatic/semi-automatic post-earthquake probabilistic risk assessment is funded by (i) the EQC Biennial Grants Programme 2010 (project 10/592), (ii) a cooperative agreement with the University of Colorado at Boulder funded by the USGS (award number G10AC00100), and (iii) in-kind research efforts from GNS Science, the University of Colorado at Boulder, and the USGS.

This paper was reviewed by Prof. John van de Lindt of The University of Alabama, Dr. Edward Field of the USGS, and Mr. David Perkins of the USGS. We sincerely appreciate their comments.

REFERENCES

American Society of Civil Engineers 2010. *Minimum Design Loads for Buildings and Other Structures, ASCE/SEI 7-10*. Reston, Virginia: ASCE.

Applied Technology Council 1978. *Tentative Provisions for the Development of Seismic Regulations for Buildings, ATC 3-06*. Palo Alto, California: ATC.

Applied Technology Council 2009. *Quantification of Building Seismic Performance Factors, FEMA P-695*. Washington, DC: Federal Emergency Management Agency.

Bazzurro, P., Cornell, C.A., Menun, C., Motahari, M. & Luco, N. 2006. *Advanced Seismic Assessment Guidelines, PEER Report 2006/05*. Berkeley, California: Pacific Earthquake Engineering Research Center.

Building Seismic Safety Council 2009. *NEHRP Recommended Seismic Provisions for New Buildings and Other Structures, FEMA P-750*. Washington, DC: Federal Emergency Management Agency.

Cornell, C.A. 1968. Engineering Seismic Risk Analysis, *Bulletin of the Seismological Society of America*, 58(5): 1583-1606.

International Code Council 2012. *International Building Code*. Falls Church, Virginia: ICC.

Luco, N. B.R. Ellingwood, R.O. Hamburger, J.D. Hooper, J.K. Kimball & Kircher, C.A. 2007. Risk-Targeted versus Current Seismic Design Maps for the Conterminous United States. *Proceedings of the Structural Engineers Association of California 76th Annual Convention.*

McGuire, R.K. 2004. *Seismic Hazard and Risk Analysis*. Oakland, California: EERI.

Ryu, H., Luco, N., Uma, S.R. & Liel, A.B. 2011. Developing fragilities for mainshock-damaged structures through incremental dynamic analysis. *9PCEE Paper No. 225.*

Ryu, H., Luco, N. & Baker, J.W. 2011. Collapse Fragility Curves for Generic Building Types. In preparation for publication in *Earthquake Spectra*.

Yeo, G.L. & Cornell, C.A. 2005. *Stochastic Characterization and Decision Bases under Time-Dependent Aftershock Risk in Performance-Based Earthquake Engineering, PEER Report 2005/13*.

Gerstenberger, M., Wiemer, S. & Jones, L. 2004. *Real-time Forecasts of Tomorrow's Earthquakes in California: A New Mapping Tool, USGS Open-File Report 2004-1390.*

Gerstenberger, M., Uma, S.R. & Luco, N. 2008. Calculation of damage state exceedance probabilities from aftershocks. *2008 NZSEE Conference Poster*.